

Energy & Environmental Science

Accepted Manuscript



This is an *Accepted Manuscript*, which has been through the Royal Society of Chemistry peer review process and has been accepted for publication.

Accepted Manuscripts are published online shortly after acceptance, before technical editing, formatting and proof reading. Using this free service, authors can make their results available to the community, in citable form, before we publish the edited article. We will replace this *Accepted Manuscript* with the edited and formatted *Advance Article* as soon as it is available.

You can find more information about *Accepted Manuscripts* in the [Information for Authors](#).

Please note that technical editing may introduce minor changes to the text and/or graphics, which may alter content. The journal's standard [Terms & Conditions](#) and the [Ethical guidelines](#) still apply. In no event shall the Royal Society of Chemistry be held responsible for any errors or omissions in this *Accepted Manuscript* or any consequences arising from the use of any information it contains.

Fast cascade neutralization of an oxidized sensitizer by an in situ-generated ionic layer of I^- species on a nanocrystalline TiO_2 electrode

Cite this: DOI: 10.1039/x0xx00000x

Received 00th January 2012,
Accepted 00th January 2012

DOI: 10.1039/x0xx00000x

www.rsc.org/

Jongchul Lim, Taewan Kim and Taiho Park*

We report a novel way to accelerate the rate of oxidized sensitizer neutralization on nanocrystalline TiO_2 electrode surfaces using a novel coadsorbent, 3,4,5-tris-butenyloxy benzoic acid (**TD**), having three terminal double bonds. 1H NMR and contact angle measurements revealed that the terminal double bonds reacted with I_2 to form an in situ-generated ionic layer of I^- species. Transient absorption spectroscopy (TAS) and electrochemical impedance spectroscopy (EIS) studies demonstrated that I^- species neighbouring the cationic dye molecules (D^+) accelerate the neutralization (or regeneration) rate (k_{D^+}), as well as decrease the recombination reactions of photoinduced electrons with D^+ (k_1) and I_3^- (k_2). Dye-sensitized solar cells treated with **TD** exhibit 10.2 % of power conversion efficiency, 22% higher due to the simultaneous improvements in J_{SC} and V_{OC} , even at 15% low dye loading levels, compared to the values obtained from a conventional device.

Broader context

The rate of oxidized sensitizer neutralization is considered as a rate-determining step among the many electrochemical reactions at the interfaces of TiO_2 / sensitizers (D) / electrolytes (redox species) in dye-sensitized solar cells. Therefore, the faster rate of oxidized sensitizer neutralization might lead an improved light harvesting, resulting in a highly efficient dye-sensitized solar cell. Here, a new concept to accelerate the rate of oxidized sensitizer neutralization is constructed using in situ-generated ionic layer of I^- species on a nanocrystalline TiO_2 electrode. The estimated regeneration time of the our device is one order of magnitude shorter than the control device, demonstrating that in situ-generated I^- participated in the regeneration of D^+ . Our novel concept has not been tried by others, although a variety of coadsorbents have been tested in the context of the sensitization process. This work emphasizes the importance of understanding and engineering the interfaces in DSCs and will provide insights into various optoelectronic fields.

Introduction

Dye-sensitized solar cells (DSCs) are based on a nanoscale-crystalline TiO_2 layer covered with dyes and capable of harvesting sun light.¹ As shown in Fig. 1(a), many photo- and electrochemical reactions take place at the interfaces between the nanoscale TiO_2 crystals, the dyes, and the electrolyte, which includes redox species, such as I^- and I_3^- .²⁻³ Understanding and engineering such interfaces are a key approach

to improving the photovoltaic performances of DSCs.⁴⁻⁵ Upon light absorption, the excited dye (D^*) injects an electron (e^-) into the conduction band (E_{CB}) of TiO_2 (k_{inj}), producing an oxidized dye (D^+) that is subsequently neutralized by I^- (k_{D^+}). The injected electron may diffuse to the surface states below the E_{CB} of the TiO_2 electrode and will recombine with oxidized species, such as D^+ or I_3^- (k_1 and k_2), resulting in the decreased charge collection efficiency (η_{cc}). Katoh

and Haque, independently, reported^{1a,6} that the dye-regeneration rate (k_{D^+}) is $\sim\mu\text{s}$ time scale which is much longer than the electron injection rate ($k_{inj} \sim > \text{ps}$). Meanwhile, the recombination rates (k_1 and k_2) with D^+ or I_3^- are in the range of $\sim 1 \text{ ms}$.^{6,7} Therefore, the dye-regeneration process ($\sim k_{D^+}$) could be considered as a rate-determining step in the electrochemical reactions. In turn, the faster k_{D^+} might lead the less recombination of the photoinduced electrons with D^+ or I_3^- (Figure 1(b)). Increasing concentration of redox species could enhance the recombination process, but, resulting in the decreasing open circuit voltage (V_{OC}) values.^{7,8}

The short circuit current density (J_{SC}) is typically estimated using the equation⁹ $J_{SC} \propto \eta_{lh} \times \eta_{inj} \times \eta_{cc} \times \eta_{reg}$ (η_{lh} : the light harvesting efficiency, η_{inj} : the electron injection efficiency from an D^* into the E_{CB} of TiO_2 , η_{reg} : the regeneration efficiency of D^+ by redox couple.) The value of η_{inj} is influenced by the energy gap between the energy levels of the lowest unoccupied molecular orbital (LUMO) of D and the E_{CB} of TiO_2 , as well as by the dye adsorption mode or the presence of aggregates at the TiO_2 electrode surfaces.¹⁰ Assuming that the values of η_{inj} do not vary significantly for a given device preparation process, J_{SC} is proportional to, first, the quantity and light harvesting efficiency (η_{lh}) of D and, secondly, the regeneration process (η_{reg}). To this end, we hypothesized that if the presence of I^- species neighboring the D^+ species were ensured by forming an ionic layer on the TiO_2 surface at an equilibrium state, then the dye-regeneration reaction (η_{reg}) efficiently would improve, thereby facilitating the light harvesting process (η_{lh}) by accelerating the regeneration rate (k_{D^+}), which also minimizes k_1 and k_2 .

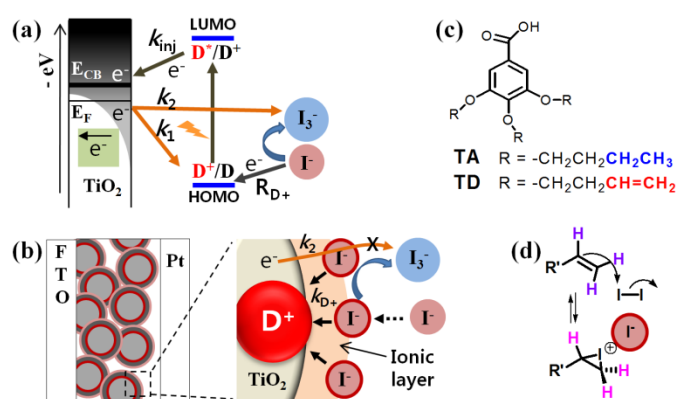


Fig. 1 (a) Electron transfer processes at the heterogeneous interface of a dye-sensitized solar cell. (b) Illustration of an ionic layer and its role on the surface of TiO_2 . (c) Chemical structures of TA and TD (Fig. S1). (d) Reversible iodization on a terminal olefin.

Here, we demonstrate the enhancement of the light harvesting process by accelerating k_{D^+} . We synthesized a novel coadsorbent, 3,4,5-tris-butenyloxy benzoic acid (TD) having three terminal double bonds (Fig. 1(c); 3,4,5-tri-butoxy benzoic acid (TA) without double bonds), which is capable of forming an ionic layer on the TiO_2 electrode surfaces (Fig. 1(b)) through the reversible iodization process (Fig. 1(d)). It is noticed that our novel concept has not been tried by others, although a variety of coadsorbents have been tested in the context of the sensitization process.¹¹

Experimental Section

3,4,5-Tributoxy benzoic acid (TA).

Synthesis of 3,4,5-tributoxy benzoic acid methyl ester (1). 1-Bromo-butane (1.37 g, 10 mmol) was added to a suspension of methyl 3,4,5-trihydroxy benzoate (0.506 g, 2.75 mmol), K_2CO_3 (5.28 g, 40 mmol), KI (0.2 g, 1.2 mmol) and 4A° molecular sieves in dry butanone (50 mL), and the mixture was heated under reflux for 3 days. The reaction mixture was filtered and the butanone distilled off. The crude product was purified by column chromatography (SiO_2 , E.A./hexane = 1/9 v/v), yielding white powder (0.775 g, 2.2 mmol, 80%). $^1\text{H NMR}$ (400 MHz, CDCl_3): δ (ppm) = 7.27 (s, 2H), 4.03 (m, 6H), 3.89 (s, 3H), 1.81 (m, 6H), 1.53 (m, 6H), 0.98 (t, $J = 7.3 \text{ Hz}$, 9H).

Synthesis of 3,4,5-tributoxy benzoic acid (TA). Compound 1 (0.775 g, 2.2 mmol) was dissolved in THF (8 mL) and methanol (50 mL). A solution of KOH (0.9 g, 15 mmol) in water (5 mL) was then added dropwise to the mixture with stirring. The mixture was stirred at room temperature for overnight, followed by reflux for 4 h. The solvents were evaporated and ice/water (30 mL) was added to the residue. The mixture was acidified with HCl conc. until pH = 3 and the product was filtered off, washed with water and then with hexane (0.67 g, 1.98 mmol, 90%). $\text{C}_{19}\text{H}_{30}\text{O}_5$; $M = 340.4$, $^1\text{H NMR}$ (400 MHz, DMSO): δ (ppm) = 7.19 (s, 2H), 3.98 (m, 6H), 1.70 (m, 6H), 1.46 (m, 6H), 0.930 (m, 9H).

3,4,5-tris-butenyloxy benzoic acid (TD).

Synthesis of 3,4,5-tris-butenyloxy benzoic acid methyl ester (2). 1-Bromo-butene (1.35 g, 10 mmol) was added to a suspension of methyl 3,4,5-trihydroxybenzoate (0.506 g, 2.75 mmol), K_2CO_3 (5.28 g, 40 mmol), KI (0.2 g, 1.2 mmol) and 4A° molecular sieves in dry butanone (50 mL), and the mixture was heated under reflux for 3 days. The reaction mixture was filtered and the butanone distilled off. The crude product was purified by column chromatography (SiO_2 , E.A./hexane = 1/9) yielded white powder (0.823 g, 2.34 mmol, 85%). $^1\text{H NMR}$ (400 MHz, CDCl_3): δ (ppm) = 7.27 (s, 2H), 5.92 (m, 3H), 5.12 (m, 6H), 4.08 (m, 6H), 3.89 (s, 3H), 2.57 (m, 6H).

Synthesis of 3,4,5-tris-butenyloxy benzoic acid (TD). Compound 2 (0.823 g, 2.34 mmol) was dissolved in THF (8 mL) and

methanol (50 mL). A solution of KOH (0.9 g, 15 mmol) in water (50 mL) was then added dropwise to the mixture with stirring. The mixture was stirred at room temperature, overnight, followed by reflux for 4 h. The solvents were evaporated and ice/water (30 mL) was added to the residue. The mixture was acidified with HCl conc. until pH = 3 and the product was filtered off, washed with water and then with hexane (0.712 g, 2.106 mmol, 90%). $C_{19}H_{24}O_5$; $M=334.4$, 1H NMR (400 MHz, DMSO): δ (ppm) = 7.21 (s, 2H), 5.91 (m, 3H), 5.14 (m, 6H), 4.01 (m, 6H), 2.34 (m, 6H).

Fabrication of DSCs. The nanocrystalline TiO_2 electrode was immediately immersed in the dye solution at room temperature for 18 h. The dye solution consisted of 0.3 mM N719 in acetonitrile and tert-butyl alcohol (1:1 v/v). The coadsorbents, **TA** or **TD**, were introduced to the dye solution at constant concentrations (0.3 mM). Coadsorbents were introduced to the dye solutions by transferring appropriate volumes of a 6 mM stock solution to yield the desired final concentrations. The counter electrode was prepared by introducing two holes, using a sandblasting drill, in the FTO glass substrate. The substrate was subsequently washed using the washing method described above. The Pt paste was pasted onto the predrilled FTO glass and subsequently sintered using the programmed heating procedure. The dye-coated photoanode and the counter electrode were assembled and sealed as a sandwich using a transparent 60 μ m thick Surlyn spacer (DuPont) by hot pressing. The interelectrode space was filled with the electrolyte solution through the predrilled hole in the counter electrode surface, and the holes were covered with the Surlyn sheet and a thin cover glass followed by heating. The electrolyte consisted of 0.6 M BMII, 0.06 M I_2 , 0.1 M guanidinium thiocyanate, 0.5 M LiI, and 0.5 M 4-*tert*-butylpyridine in a mixture of acetonitrile and valeronitrile (85:15 v/v). More details are included in the electronic supplementary information.

Transient absorption spectrophotometer. Pulsed laser excitation was applied using Continuum Surelite-II Q-switched Nd:YAG laser ($\lambda=355$ nm, 10 Hz repetition rate). The output of the optical parametric oscillator (OPO, pulse width at half-height 5 ns) was tuned at 532 nm and attenuated to 75 μ J/cm²-pulse. The analyzer light, produced by a 150 W Xe arc lamp, was passed through the sample, and was detected by the amplifier equipped Si photodiode. A 1 GHz band-pass digital signal analyzer was employed to record the time course of the optical absorbance changes induced by laser excitation of the films. Satisfactory signal-to-noise ratios were typically obtained by averaging over 512 laser shots.

Results and Discussion

The iodization process was monitored by 1H NMR, using 1-hexene as a model compound. The olefinic active site in 1-hexene provided three peaks, H_a and two diastereotopic H_b and H_c peaks (Fig. 2(a)).

The addition of I_2 to the 1-hexene solution (*d*-chloroform) generated three new peaks (H_{a1} , H_{b1} , and H_{c1}), in addition to the peaks corresponding to 1-hexene at equilibrium. The latter pattern was identical to the peaks provided by propylene oxide, indicating that the two protons (H_b and H_c) retained their diastereotopic environments (see Supporting information for details, Fig. S2). In *d*-acetonitrile solution, further reactions were expected, as *d*-acetonitrile is competitive and contains greater amounts of water molecules than *d*-chloroform; however, indistinguishable results were obtained in *d*-acetonitrile and *d*-chloroform, after the removal of residual water (Fig. 2(b) and Fig. S3). Interestingly, the presence of water shifted the peak positions of the diastereotopic protons (H_{b1} and H_{c1}) (see Supporting information for details, Fig. S4), which were more exposed to water molecules than H_{a1} , down-field. The positive charge on I^+ would then have been stabilized by dispersing the charges across the carbon atom connected to H_{b1} and H_{c1} (Fig. S5).

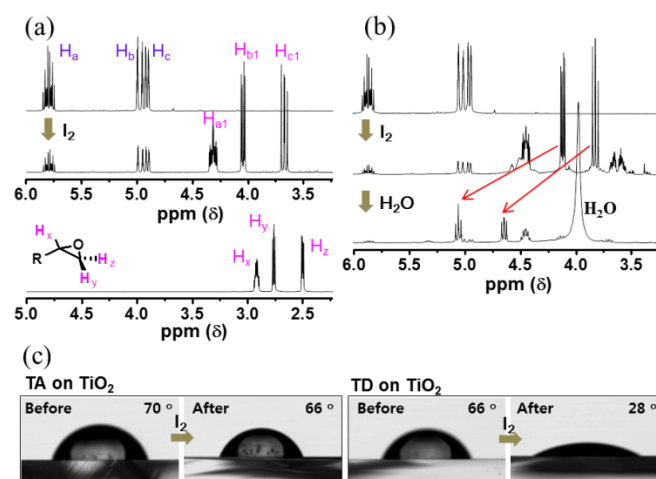


Fig. 2 1H NMR spectra of (a) 1-hexene without or with I_2 (1 eq.) and propylene oxide in *d*-chloroform, or (b) 1-hexene without or with I_2 (1 eq.), after further additions of water to the *d*-acetonitrile solution. (c) Water contact angle before and after iodization of **TA** and **TD** anchored on the TiO_2 substrate surfaces.

Water contact angle (θ_c) measurements supported the conclusion that ionic complexes were generated at the double bonds of **TD**, as shown in Fig. 2(c) (see also Fig. S6). Unlike the case of **TA**, the θ_c value for the TiO_2 electrode covered with **TD**, after treatment with a dried acetonitrile (AN) solution containing I_2 and KI, decreased significantly from 66 to 28°. This result indicated that the double bonds reacted with I_2 and were then solvated with water, consistent with the 1H NMR experiments.

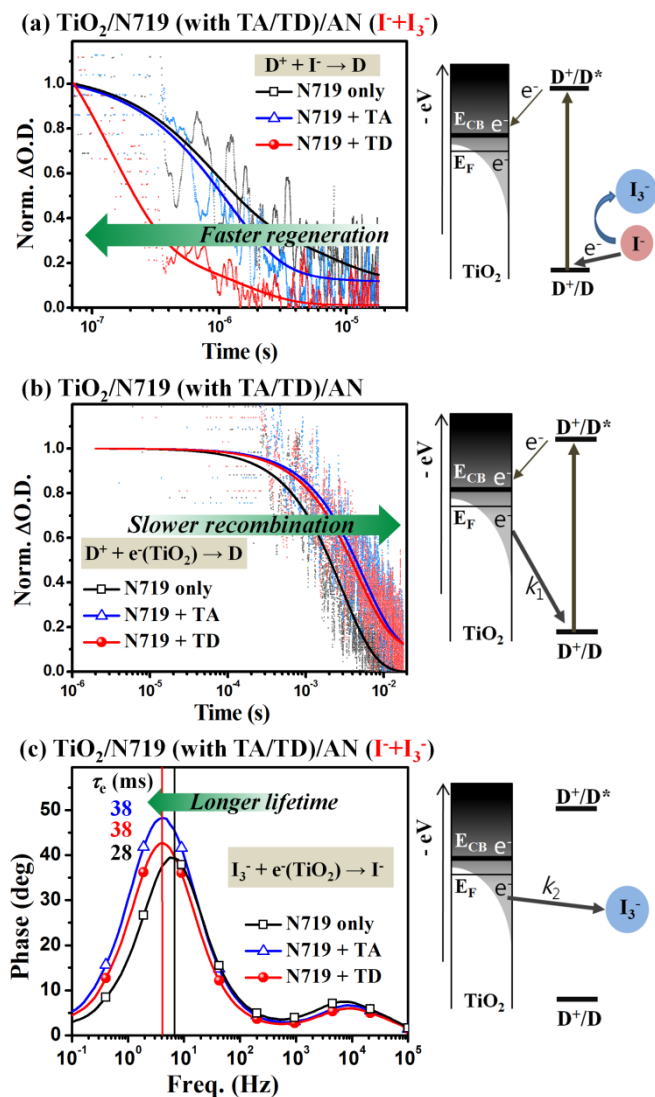


Fig. 3 Normalized decay profiles of D^+ in devices prepared with **TA** or **TD** (N719+**TA** or N719+**TD**), in comparison with the control device (N719-only), probed at 790 nm using transient absorption spectroscopy in the presence (a) or absence (b) of redox species. The 790 nm absorption profile examined the metal-to-ligand charge transfer (MLCT) transition associated with the ligand-localized D^+ ,^{10a} upon excitation at 532 nm (the maximum absorption of the N719 dye) (Fig. S7). (c) Bode plots obtained from devices prepared with **TA** or **TD** (N719+**TA** or N719+**TD**), in comparison with the control device (N719-only), using electrochemical impedance spectroscopy under dark conditions in the vicinity of V_{oc} (0.63 V) (Fig. S8).

We examined the rapid regeneration of D^+ by the ionic complexes, including I^- . The rate of dye regeneration (ca. $\sim 10^6/s$) typically exceeds the recombination reaction rates (ca. $\sim 10^3/s$);^{1b,6} therefore, in the presence of redox species, most D^+ species could be regenerated by I^- .^{10a} Fig. 3(a) shows the normalized decay profiles of D^+ probed at 790 nm using TAS ($D^+ + e^- \rightarrow D$). The estimated regeneration time at

0.5 $\Delta O.D.$ for $TiO_2/N719$ (with **TD**)/AN ($I^- + I_3^-$) was $0.2 \pm 0.03 \mu s$, one order of magnitude shorter than those for $TiO_2/N719$ (with **TA**)/AN ($I^- + I_3^-$) or the control device, demonstrating that in situ-generated I^- on **TD** participated in the regeneration of D^+ .

The **TA** and **TD** coadsorbents could have formed a physical barrier, which would be expected to increase the interfacial resistance at the TiO_2/D /electrolyte interface and decrease k_1 and k_2 , as has been observed previously.^{4c,11c,12} The effects of the coadsorbents on k_1 and k_2 were characterized using TAS^{1d,8,13} and electrochemical impedance spectroscopy (EIS),^{10a} respectively. In the absence of redox species (I_3^- and I^-), the photoinduced electrons were expected to recombine with D^+ s (thus, $k_1: D^+ + e^- (TiO_2) \rightarrow D$). The estimated life time of D^+ time at 0.5 $\Delta O.D.$ in the electrodes prepared with the **TA** and **TD** coadsorbents (~ 5.0 ms) were longer than the lifetime of D^+ in the control electrode (2.5 ms) as revealed by the decay kinetics of the k_1 (Fig. 3(b)). In the presence of the electrolytes (I_3^- and I^-), the photoinduced electrons mainly recombined with I^- ($k_2: I_3^- + e^- (TiO_2) \rightarrow I^-$). The electron lifetimes ($\tau_{e,(k_2)}$) in the electrodes prepared with **TA** and **TD** (38 ms) were longer than that in the control electrode (28 ms), as shown in the bode plots (Fig. 3(c)).

Table 1. Photocurrent–voltage characteristics^[a] of devices prepared with **TA** or **TD** (N719+**TA** or N719+**TD**), or with a control device (N719 only), under AM 1.5 irradiation.

Devices	Relative [dye] ^[b]	V_{oc} [V]	J_{sc} [mA/cm ²]	FF [%]	η [%]
N719 only	1.00	0.735	16.2	69.9	8.3
N719 + TA	0.84	0.773	16.3	73.2	9.2
N719 + TD	0.85	0.783	17.7	73.2	10.2

^[a] Values obtained using the average over 4 devices, for 5 individual experiments (Fig. S9), ^[b] The values were determined by measuring UV-Vis absorption spectra (see insert in Fig. 4(a))

Finally, the role of the ionic layer in the photoelectrochemical reaction was examined in the context of device operation, as shown in Fig. 4(a) and Table 1. The quantities of N719 adsorbed onto the electrodes cosensitized with **TA** or **TD** were measured using UV-Vis spectrophotometer and were found to be 15 or 16% lower, respectively, than the quantity absorbed onto the control electrode

(N719 only, see insert in Fig. 4(a)), indicating that N719 and the coadsorbents (**TA** and **TD**) competed for anchoring sites on the Ti^{4+} active sites of the nanocrystalline TiO_2 electrodes.^{11c, 11f}

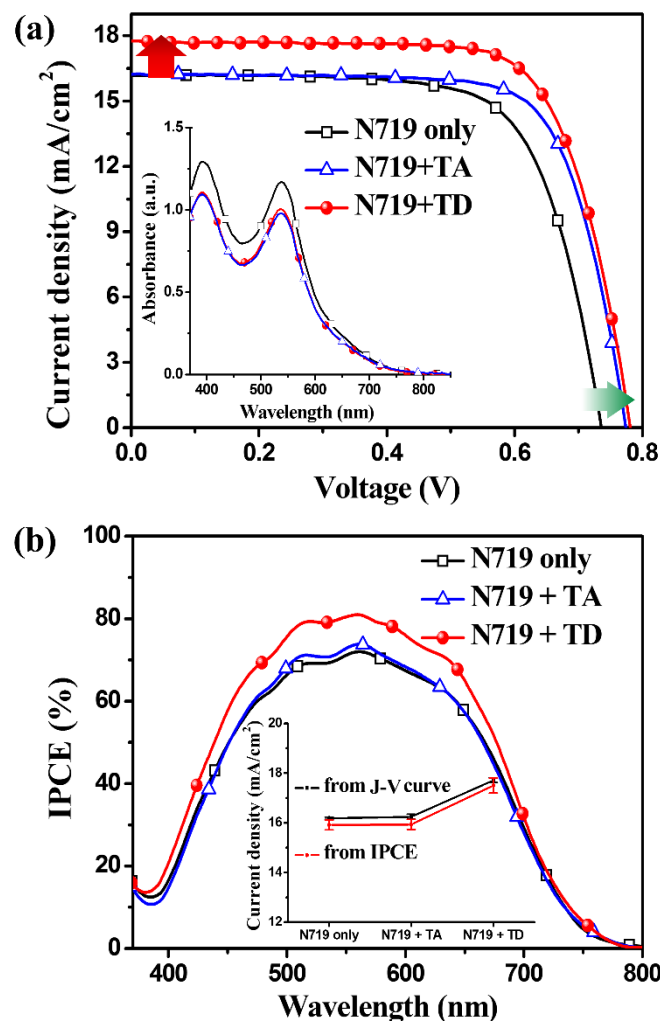


Fig. 4 (a) Representative photocurrent–voltage curves and (b) incident photon-to-current efficiency (IPCE) spectra for devices prepared with **TA** or **TD** (N719+**TA** or N719+**TD**), in comparison with a control device (N719 only). Insert in (a): comparison of amounts of N719 adsorbed on the TiO_2 electrodes calculated using UV-Vis spectrophotometer. Insert in (b): comparison of J_{SC} values calculated from IPCE (%) spectra and J - V curves. J - V curves measured under AM 1.5 irradiation (DSCs: 12 μm thickness of TiO_2 and 0.078 cm^2 active areas defined using a black metal mask).

The power conversion efficiency (η) of the device prepared with **TD** was 10.2 %, 23 % improvement compared to the control device ($\eta = 8.3\%$).¹⁴ The improvement was ascribed to the increased J_{SC} as well as V_{OC} values, even in 15% low dye-loading in the device prepared with **TD**. The V_{OC} values of the devices prepared with **TA** and **TD** are *ca.* 40 mV higher than that obtained in the control device, probably

due to the increased interfacial resistance at the $\text{TiO}_2/\text{D}/\text{electrolyte}$ interface as demonstrated in the EIS experiments (Fig. 3(c)). The increased interfacial resistance could minimize the J_{SC} loss caused from the recombination reactions, resulting in the relative increase in V_{OC} according to the equation:¹⁵ $V_{OC} \sim (nkT/q) \ln(J_{SC}/J_s)$ (n : the device ideality factor, k : the Boltzmann constant, T : the temperature in Kelvin, q : the fundamental charge, J_s : the saturation current density). In addition, we measured the density-of-states (DOS) on the TiO_2 surfaces using cyclic voltammetry (Fig. S10).

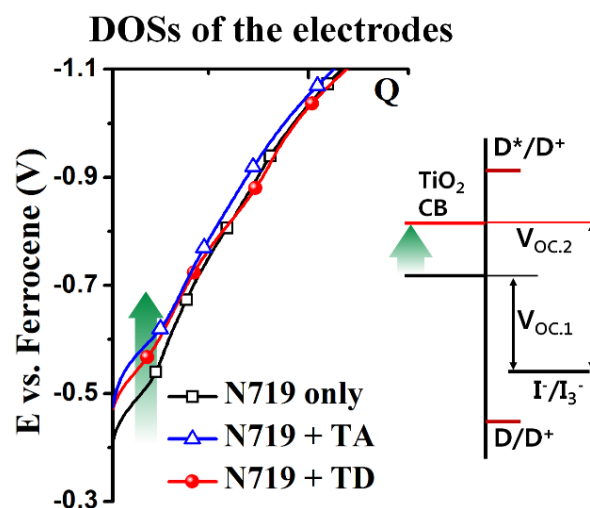


Fig. 5 The energy levels at the TiO_2 film/BMIB interface in the electrodes prepared with **TA** or **TD** (N719+**TA** or N719+**TD**), or with a control electrode (N719 only), were estimated using cyclic voltammetry using a 0.05 V/s scan rate.

As Grätzel¹⁶ and we,^{11b} independently, reported, the capacitive currents in the electrodes at the TiO_2 / 1-butyl-3-methylimidazolium bromide (BMIB)¹⁷ interface displayed gradual onsets under a forward potential. The lower-energy surface states, in which photoinduced electrons were trapped, resulted in fewer recombination reactions. The electrode prepared with **TA** and **TD** indicated that the edge of the TiO_2 conduction band was shifted *ca.* 63 mV toward the vacuum level compared to the control electrode (Fig. 5). Therefore, the coadsorbents (**TA**) present on the TiO_2 electrode surface reduced k_1 and k_2 .

The overall increase in J_{SC} (16.2 to 16.3 mA/cm^2) for the device with **TA** was negligible due to the decrease in the dye loading level by 16%, in spite of the less recombination. On the other hand, the device prepared with **TD** exhibited an increase in J_{SC} (16.2 to 17.7 mA/cm^2) as well as V_{OC} (0.735 to 0.783 V). We also confirmed the tendency in a thinner TiO_2 active layer (Fig. S11). Highly ionic coadsorbents

(e.g., 4-guanidinobutyric^{11b} or chenodeoxycholic acid¹⁸) have been tested previously, but these coadsorbents only increased either the V_{OC} or J_{SC} value. The increase in J_{SC} as well as V_{OC} , as observed in the device prepared with **TD**, could not be ascribed to the ionic character or the alcohol groups generated by scavenging water molecules. We verified the J_{SC} values of the devices by comparison with the calculated J_{SC} values obtained from the incident photon-to-current efficiency (IPCE) spectra (Fig. 4(b)).¹⁹ Therefore, we concluded that the dye regeneration reaction ($\sim\eta_{reg}$) occurred efficiently through the reaction between the I^- species generated on **TD** and D^+ , thereby facilitating the light harvesting process ($\sim\eta_h$), even at a low dye loading level.

Conclusions

we demonstrated that **TD**, which includes three terminal double bonds, reacted with I_2 and generated ionic complexes on the surfaces of a TiO_2 electrode. The in situ-generated ionic layer accelerated the neutralization (or regeneration) rate (k_{D^+}) of D^+ and decreased the recombination reactions with D^+ (k_1) and I_3^- (k_2) due to coadsorbent effects. The device cosensitized with **TD** provided 10.2 % of power conversion efficiency, 22% higher due to the simultaneous improvements in J_{SC} and V_{OC} , even at 15% low dye loading levels, compared to the values obtained from a conventional device under identical experimental conditions. This work demonstrated the importance of understanding and engineering the interfaces between nanoscale TiO_2 crystals, dyes, and electrolytes at the molecular level and will provide insights into various optoelectronic fields.

Acknowledgements

This work was supported by grants from the Nano Material Technology Development Program (2012M3A7B4049989), the Center for Next Generation Dye-Sensitized Solar Cells (No. 2008-0061903), and the Center for Advanced Soft Electronics under the Global Frontier Research Program (Code No. NRF-2012M3A6A5055225) through the National Research Foundation of Korea (NRF) by the MSIP, Korea.

Notes and references

* Corresponding author: Pohang University of Science and Technology (POSTECH), San 31, Nam-gu, Pohang, Kyungbuk, Korea. Fax: 82-54-279-8298; Tel: 82-54-279-2394; E-mail: taihopark@postech.ac.kr

Electronic Supplementary Information (ESI) available: [Experimental details, Extra 1H NMR spectra, EIS spectra, cyclic voltammograms and $J-V$ characteristics for 7.0 μm TiO_2 thicknesses]. See DOI: 10.1039/b000000x/

- a) B. C. O'Regan and M. Grätzel, *Nature*, 1991, **353**, 737.; b) R. Katoh, A. Furube, A. V. Barzykin, H. Arakawa and M. Tachiya, *Coord. Chem. Rev.*, 2004, **248**, 1195; c) A. Hagfeldt, G. Boschloo, L. Sun, L. Kloo and H. Pettersson, *Chem. Rev.*, 2010, **110**, 6595; d) J. Luo, M. Xu, R. Li, K. W. Huang, C. Jiang, Q. Qi, W. Zeng, J. Zhang, C. Chi, P. Wang and J. Wu, *J. Am. Chem. Soc.*, 2014, **136**, 265; e) A. Y. Anderson, P. R. F. Barnes, J. R. Durrant and B. C. O'Regan, *J. Phys. Chem. C*, 2011, **115**, 2439.
- S.-H. Park, I. Y. Song, J. Lim, Y. S. Kwon, J. Choi, S. Song, J.-R. Lee and T. Park, *Energy Environ. Sci.*, 2013, **6**, 1559.
- a) J. Wang, I. Mora-Sero, Z. Pan, K. Zhao, H. Zhang, Y. Feng, G. Yang, X. Zhong and J. Bisquert, *J. Am. Chem. Soc.*, 2013, **135**, 15913; b) P. V. Kamat, *Chem. Rev.*, 1993, **93**, 267; c) H. Imahori, T. Umeyama and S. Ito, *Acc. Chem. Res.*, 2009, **42**, 1809.
- a) F. Sauvage, J. D. Decoppet, M. Zhang, S. M. Zakeeruddin, P. Comte, M. Nazeeruddin, P. Wang and M. Grätzel, *J. Am. Chem. Soc.*, 2011, **133**, 9304; b) H. J. Snaith, *Adv. Funct. Mater.*, 2010, **20**, 13; c) S. N. Mori, W. Kubo, T. Kanzaki, N. Masaki, Y. Wada and S. Yanagida, *J. Phys. Chem. C*, 2007, **111**, 3522.
- a) Y. S. Kwon, J. Lim, H.-J. Yun, Y.-H. Kim and T. Park, *Energy Environ. Sci.*, 2014, **7**, 1454; b) I. Y. Song, Y. S. Kwon, J. Lim and T. Park, *ACS Nano*, 2014, DOI: 10.1021/nn5016083; c) Y. S. Kwon, J. Lim, I. Y. Song, W.-S. Shin, S.-J. Moon and T. Park, *J. Mater. Chem.*, 2012, **22**, 8641; d) Y. S. Kwon, I. Song, J. Lim, I. Y. Song, A. Siva and T. Park, *ACS Appl. Mater. Interfaces*, 2012, **4**, 3141.
- S. Haque, Y. Tachibana, D. R. Klug and J. R. Durrant, *J. Phys. Chem. B*, 1998, **102**, 1745.
- G. Boschloo and A. Hagfeldt, *Acc. Chem. Res.*, 2009, **42**, 1819.
- S.-H. Park, J. Lim, Y. S. Kwon, I. Y. Song, J. M. Choi, S. Song, T. Park, *Adv. Energy Mater.*, 2013, **3**, 184.
- C. S. Kley, C. Dette, G. Rinke, C. E. Patrick, J. Cechal, S. J. Jung, M. Baur, M. Durr, S. Rauschenbach, F. Giustino, S. Stepanow and K. Kern, *Nano letters*, 2014, **14**, 563.
- a) S.-H. Park, J. Lim, I. Y. Song and T. Park, *Adv. Energy Mater.*, 2014, **4**, 1300489; b) H. J. Son, X. Wang, C. Prasittichai, N. C. Jeong, T. Aaltonen, R. G. Gordon and J. T. Hupp, *J. Am. Chem. Soc.*, 2012, **134**, 9537; c) F. Fabregat-Santiago, J. Bisquert, G. Garcia-Belmonte, G. Boschloo and A. Hagfeldt, *Sol. Energ. Mat. Sol. Cells*, 2005, **87**, 117.
- a) Z. Zhang, S. M. Zakeeruddin, B. C. O'Regan, R. Humphry-Baker and M. Grätzel, *J. Phys. Chem. B*, 2005, **109**, 21818; b) J. Lim, Y. S. Kwon and T. Park, *Chem. Commun.*, 2011, **47**, 4147; c) S.-H. Park, J. Lim, I. Y. Song, N. Atmakuri, S. Song, Y. S. Kwon, J. M. Choi and T. Park, *Adv. Energy Mater.*, 2012, **2**, 219; d) Q. J. Yu, Y. H. Wang, Z. H. Yi, N. N. Zu, J. Zhang, M. Zhang and P. Wang, *ACS Nano*, 2010, **4**, 6032; e) A. Kay and M. Graetzel, *J. Phys. Chem.*, 1993, **97**, 6272; f) J. Lim, Y. S. Kwon, S. H. Park, I. Y. Song, J. Choi and T. Park, *Langmuir*, 2011, **27**, 14647; g) E.-H. Kong, J. Lim, Y.-J. Chang, Y.-H. Yoon, T. Park and H. M. Jang, *Adv. Energy Mater.*, 2013, **3**, 1344.
- P. Wang, S. M. Zakeeruddin, R. Humphry-Baker, J. E. Moser and M. Grätzel, *Adv. Mater.*, 2003, **15**, 2101.
- L. J. A. Koster, V. D. Mihailetschi, R. Ramaker and P. W. M. Blom, *Appl. Phys. Lett.*, 2005, **86**, 123509.
- Notice that the control value ($\eta = 8.3\%$) is still greater than those ($\eta = 6 \sim 8\%$) reported in literatures in the identical condition employing 12 \sim 15 μm thickness of TiO_2 and N719 sensitizer. a) M. Kimura, H. Nomoto, N. Masaki and S. Mori, *Angew. Chem. Int. Ed.*, 2012, **51**,

- 4371; b) M. Cheng, X. Yang, F. Zhang, J. Zhao and L. Sun, *Angew. Chem. Int. Ed.*, 2012, **51**, 9896; c) A. Reynal, A. Forneli and E. Palomares, *Energy Environ. Sci.*, 2010, **3**, 805.
- 15 S. Y. Huang, G. Schlichthörl, A. J. Nozik, M. Grätzel and A. J. Frank *J. Phys. Chem. B*, 1997, **101**, 2576.
- 16 Z. Zhang, S. M. Zakeeruddin, B. C. O'Regan, R. Humphry-Baker and M. Grätzel, *J. Phys. Chem. B*, 2005, **109**, 21818.
- 17 Q. Tai, X. Zhao and F. Yan, *J. Mater. Chem.*, 2010, **20**, 7366.
- 18 J. H. Yum, S. J. Moon, R. Humphry-Baker, P. Walter, T. Geiger, F. Nüesch, M. Grätzel and Md K. Nazeeruddin. *Nanotechnology*, 2008, **19**, 424005.
- 19 X.-Z. Guo, Y.-H. Luo, C.-H. Li, D. Qin, D.-M. Li and Q.-B. Meng, *Curr. Appl. Phys.*, 2012, **12**, e54.

The table of contents

A novel coadsorbent which includes three terminal double bonds, reacted with I_2 and generated ionic complexes on the surfaces of a TiO_2 electrode. The *in situ*-generated ionic layer accelerated the neutralization rate of dye^+ and decreased the recombination reactions with dye^+ and I_3^- due to coadsorbent effects, resulting in the 22% higher power conversion efficiency (η), even at 15% low dye loading levels, compared to the values obtained from a conventional device.

Keyword

Dye-sensitized solar cells • Iodization on olefin • Rate-determining step • Neutralization • Transient absorption spectroscopy

Jongchul Lim, Taewan Kim, and Taiho Park *

Fast cascade neutralization of an oxidized sensitizer by an in situ-generated ionic layer of I^- species on a nanocrystalline TiO_2 electrode

TOC figure

